Tiam1-regulated osteopontin in senescent fibroblasts contributes to the migration and invasion of associated epithelial cells

Jiewei Liu[1,2], Kun Xu[1], Maya Chase[1,3], Yuxin Ji[1], Jennifer K. Logan[1,4] and Rachel J. Buchsbaum[1,4,5,*]

[1]Molecular Oncology Research Institute, Tufts Medical Center Boston, MA 02111, USA
[2]Department of Oncology, West China Hospital, Sichuan University, Chengdu, Sichuan, 610041, China
[3]Bucknell University, Lewisburg, PA, 17837, USA
[4]Tufts University School of Medicine, Boston, MA, 02111, USA
[5]Department of Medicine, Tufts Medical Center, Boston, MA, 02111, USA
*Author for correspondence (rbuchsbaum@tuftsmedicalcenter.org)

Accepted 12 August 2011
Journal of Cell Science 125, 376–386

doi: 10.1242/jcs.089466

Summary

The tumor microenvironment undergoes changes concurrent with neoplastic progression. Cancer incidence increases with aging and is associated with tissue accumulation of senescent cells. Senescent fibroblasts are thought to contribute to tumor development in aging tissues. We have shown that fibroblasts deficient in the Rac exchange factor Tiam1 promote invasion and metastasis of associated epithelial tumor cells. Here, we use a three-dimensional culture model of cellular invasiveness to outline several steps underlying this effect. We find that stress-induced senescence induces decreased fibroblast Tiam1 protein levels and increased osteopontin levels, and that senescent fibroblast lysates induce Tiam1 protein degradation in a calcium- and calpain-dependent fashion. Changes in fibroblast Tiam1 protein levels induce converse changes in osteopontin mRNA and protein. Senescent fibroblasts induce increased invasion and migration in co-cultured mammary epithelial cells. These effects in epithelial cells are ameliorated by either increasing fibroblast Tiam1 or decreasing fibroblast osteopontin. Finally, in seeded cell migration assays we find that either senescent or Tiam1-deficient fibroblasts induce increased epithelial cell migration that is dependent on fibroblast secretion of osteopontin. These findings indicate that one mechanism by which senescent fibroblasts promote neoplastic progression in associated tumors is through degradation of fibroblast Tiam1 protein and the consequent increase in secretion of osteopontin by fibroblasts.

Key words: Tiam1, Osteopontin, Senescence, Tumor microenvironment, Invasion, Migration

Introduction

It is increasingly recognized that the tumor microenvironment plays an important role in the development of cancers. Tumor-associated stroma undergo intracellular and extracellular changes concurrent with neoplastic progression. The incidence of most human cancers increases with age, and aging is associated with accumulation of senescent cells in replicating tissues (Campisi, 2005). Cellular senescence, first defined as the process limiting the proliferative potential of normal human cells, is characterized by permanent growth arrest, resistance to apoptosis and changes in gene expression, with consequent secretion of factors that disrupt the surrounding tissue architecture (Hayflick, 1965; Krtolica and Campisi, 2002). Significant work suggests that senescent fibroblasts contribute to tumor development in aging tissues (Krtolica et al., 2001; Krtolica and Campisi, 2002; Castro et al., 2003; Yang et al., 2006; Kang et al., 2008). Different stresses can induce cellular senescence, including telomere shortening, DNA damage by radiation or oxidants, disruption of heterochromatin structure and strong mitogenic signals (Itahana et al., 2004). Senescent stromal cells can increase multiple neoplastic properties of associated epithelial cells, including growth, survival, epithelial–mesenchymal transition (EMT) and invasiveness (Krtolica et al., 2001; Coppe et al., 2008). In human cells, senescence is triggered through activation of p53–p21 and/or p16–Rb pathways, and the senescent phenotype in many cell types is associated with acquisition of senescence markers such as senescence-associated β-galactosidase (SA-βgal) activity, DNA damage foci and senescence-associated heterochromatic foci (Dimri et al., 1995; d'Adda di Fagagna et al., 2003; Narita et al., 2003; Ben-Porath and Weinberg, 2005). Multiple secreted factors involved in signaling between cells are increased in senescent cells, reminiscent of an inflammatory state (reviewed by Davalos et al., 2010).

Recent work has shown osteopontin (OPN) to be necessary in the promotion of pre-neoplastic cell growth by senescent fibroblasts (Pazolli et al., 2009). Senescent fibroblasts stimulated the growth of pre-neoplastic keratinocytes in cell culture and in a mouse skin tumor model. Silencing fibroblast OPN did not prevent stress-induced senescence in the fibroblasts, but did prevent induction by senescent fibroblasts of cell growth in associated keratinocytes. OPN is a phosphorylated glycoprotein secreted into the extracellular matrix by multiple cell types (Weber, 2008). In experimental systems, OPN triggers multiple processes involved in tumor cell progression, invasion and metastasis. Increased OPN expression is associated with

poorer outcomes in a wide range of human tumors (Wai and Kuo, 2008).

The effect of senescent fibroblasts in stimulating neoplastic progression of epithelial cells is reminiscent of our findings with Tiam1-deficient fibroblasts. Tiam1 is a ubiquitous Rac exchange factor that interacts with many different proteins, leading to multiple effects in cells (Buchsbaum et al., 2002; Buchsbaum et al., 2003; Mertens et al., 2003; Connolly et al., 2005; Zhang and Macara, 2006). Tiam1 functions have been most studied within the context of epithelial and endothelial cells, rather than mesenchymal cells. We have recently shown that Tiam1 silencing in fibroblasts leads to increased invasion and metastasis of associated tumor cells in several experimental models, including complex tissue culture models and a human xenograft model (Xu et al., 2010). Here we show that stress-induced senescence leads to decreased levels of fibroblast Tiam1 and that Tiam1-induced change in fibroblast OPN secretion is a mechanism underlying the effect of fibroblast Tiam1 on associated epithelial cells.

Results

Osteopontin mRNA and protein expression are inversely correlated with Tiam1 protein expression in fibroblasts

To investigate how Tiam1 expression in tumor-associated fibroblasts could affect invasiveness of associated tumor cells, we performed gene expression analysis in two groups of cell lines with altered Tiam1 expression using Affymetrix microarrays. The cell lines used were human reduction mammary fibroblasts (RMFs) with stable silencing of Tiam1 (shTiam-RMF) compared with control RMFs (C-RMF), and mouse embryo fibroblasts (MEFs) with inducible Tiam1 expression (+Tiam-MEF) compared with induced control MEFs. Genes with differential expression as a result of Tiam1 deficiency or overexpression included several cytokines and extracellular matrix proteins (supplementary material Fig. S1). To identify gene expression changes specifically resulting from changes in Tiam1, we looked for genes with corresponding inverse changes between Tiam1-silenced and Tiam1-overexpressing data sets. This approach identified the *OPN* gene, which was consistently upregulated in Tiam1-deficient fibroblasts and consistently downregulated in Tiam1-overexpressing fibroblasts. OPN is a secreted glycoprotein and many of its effects are mediated through NFκB signaling (Wai and Kuo, 2004). Consistent with this, pathway analysis also revealed overexpression in multiple NFκB pathway components in Tiam1-deficient fibroblasts and, conversely, underexpression in multiple NFκB pathway components in Tiam1-overexpressing fibroblasts (supplementary material Fig. S2). Given the association of increased OPN expression with tumor progression and metastasis (Wai and Kuo, 2008), it seemed reasonable to focus on OPN as a potential mediator of Tiam1 effects in the tumor microenvironment.

To validate the microarray findings, we first analyzed *OPN* mRNA levels in shTiam-RMF cells using quantitative real-time PCR (qRT-PCR). *OPN* mRNA was consistently upregulated in shTiam-RMF compared with C-RMF (Fig. 1A). The amount of secreted OPN was also assessed by immunoblots of conditioned media. OPN protein levels were consistently increased two- to threefold in conditioned medium from Tiam1-deficient RMF compared with control RMF (Fig. 1B).

We also tested *OPN* mRNA expression in the inducible +Tiam1-MEF line. After removal of doxycycline from culture

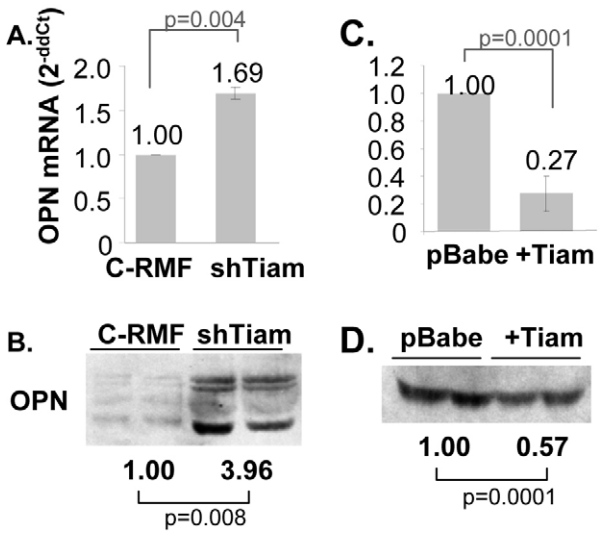

Fig. 1. OPN expression varies inversely with Tiam1 expression in fibroblasts. (**A**,**C**) Results of qRT-PCR using OPN-specific primers. Data represent mean ± s.d. for a minimum of three experiments, each done in triplicate. (**B**,**D**) Immunoblots for OPN from concentrated conditioned medium harvested from equal numbers of cells. Samples were loaded in duplicate; numbers below blots indicate quantification by densitometry for triplicate experiments. C-RMF, RMF with control viral hairpin; shTiam, Tiam1-deficient RMF; pBabe, RMF with control pBabe vector; +Tiam, Tiam1-overexpressing RMF. *P* values were derived using the Student's *t*-test.

medium, Tiam1 protein overexpression was confirmed by immunoblots (supplementary material Fig. S3A). RT-PCR using OPN-specific primers confirmed that *OPN* mRNA was significantly decreased in the presence of Tiam1 overexpression compared with doxycycline-deprived MEF-pBIG control cells (supplementary material Fig. S3B). To validate that this converse correlation also occurs in human fibroblasts, we constructed an RMF cell line with stable high expression of Tiam1 (+Tiam-RMF) (supplementary material Fig. S4B). These cells exhibited a significant decrease in *OPN* mRNA levels (Fig. 1C) as well as in secreted protein (Fig. 1D) compared with control cells. These results confirm the results of the microarray and indicate that *OPN* mRNA and protein expression are inversely correlated with Tiam1 protein expression in human fibroblasts.

RMFs undergo stress-induced senescence

Senescent fibroblasts can induce an EMT in associated tumor cells and display upregulated OPN expression (Krtolica et al., 2001; Pazolli et al., 2009). We have found that Tiam1-deficient fibroblasts induce increased invasion and metastasis in associated tumor cells (Xu et al., 2010). We therefore hypothesized that stress-induced senescence might lead to downregulation of Tiam1 in fibroblasts.

We first investigated whether our RMF cells, which are immortalized by telomerase expression, could undergo stress-induced senescence. We initially tested several different inducers, including oxidative stress (hydrogen peroxide) or sub-lethal DNA damage (using the chemotherapeutic agent bleomycin or radiation) (Aoshiba et al., 2003; Parrinello et al., 2005; Bavik et al., 2006; Hornsby, 2007). Seven days after induction, cells treated with H_2O_2, bleomycin or radiation had

taken on a morphologic appearance characteristic of senescence, appearing flattened and enlarged, and did not undergo either proliferation or apoptosis for at least 2 weeks (Krtolica and Campisi, 2002). Almost all the cells exhibited SA-βgal staining (supplementary material Fig. S5), indicating effective induction of senescence by each stress (Dimri et al., 1995). Of note, in related experiments Tiam1 silencing or overexpression did not affect induction of senescence (supplementary material Fig. S6).

Stress-induced senescence leads to inverse changes in OPN and Tiam1 in fibroblasts

We next found that OPN expression is increased in senescent RMF cells, which is similar to previous findings in senescent foreskin fibroblasts (Pazolli et al., 2009). *OPN* mRNA levels were significantly increased in cells induced to senesce by either oxidative or chemical stress (Fig. 2A). Furthermore, increases in secreted OPN were also seen in conditioned medium harvested from cells after induction of senescence by either type of stress (Fig. 2B).

We then assessed Tiam1 expression in RMFs undergoing stress-induced senescence. In contrast to the results with OPN, we found no significant difference in *Tiam1* mRNA between pre-senescent and senescent cells (Fig. 2C). However, we saw a notable decrease in Tiam1 protein in cells that had undergone either oxidative or chemical stress-induced senescence (Fig. 2D). We also tested the effect of senescence induction on cells with increased baseline Tiam1 expression using the +Tiam-RMF line. *Tiam1* mRNA was significantly higher in +Tiam1-RMF cells than in control RMF cells, and did not change with senescence induction (Fig. 2E). However, Tiam1 protein levels in these cells also decreased significantly upon senescence induction (Fig. 2F). These results indicate that stress-induced senescence leads to both increases in OPN and decreases in Tiam1 protein. Oxidative stress was used to induce senescence for the remainder of the experiments.

Tiam1 protein is probably degraded by calpain protease during stress-induced senescence in cells

The findings on *Tiam1* mRNA and protein expression suggest post-transcriptional regulation of Tiam1 in cells undergoing senescence. Several signaling pathways and proteases have been reported to be involved in the degradation of Tiam1 protein, in particular activation of calcium-dependent calpain proteases (Qi et al., 2001; Woodcock et al., 2009). Induction of senescence in various cell types triggers a DNA damage response that then triggers activation of calpain proteases (Demarchi et al., 2010). In order to explore whether calpains might be involved in Tiam1 downregulation in senescent cells, we tested whether calpain activation was increased in cells undergoing induced senescence (supplementary material Fig. S7). Although pre-senescent cells exhibited some calpain activity at baseline, this was increased over twofold in cells undergoing stress-induced senescence. We then asked whether inhibition of calpain proteases would block the decrease in Tiam1 seen in senescent cells. Treatment of cultured cells with the calpain inhibitor ALLN during induced senescence led to toxic cell death at all doses tested. Therefore, we performed an in vitro Tiam1 cleavage assay based on similar in vitro protease assays reported previously (Li et al., 1997; Juo et al., 1998; Qi et al., 2001; Woodcock et al., 2009). Tiam1 immunoprecipitates from cells with exogenous Tiam1 expression

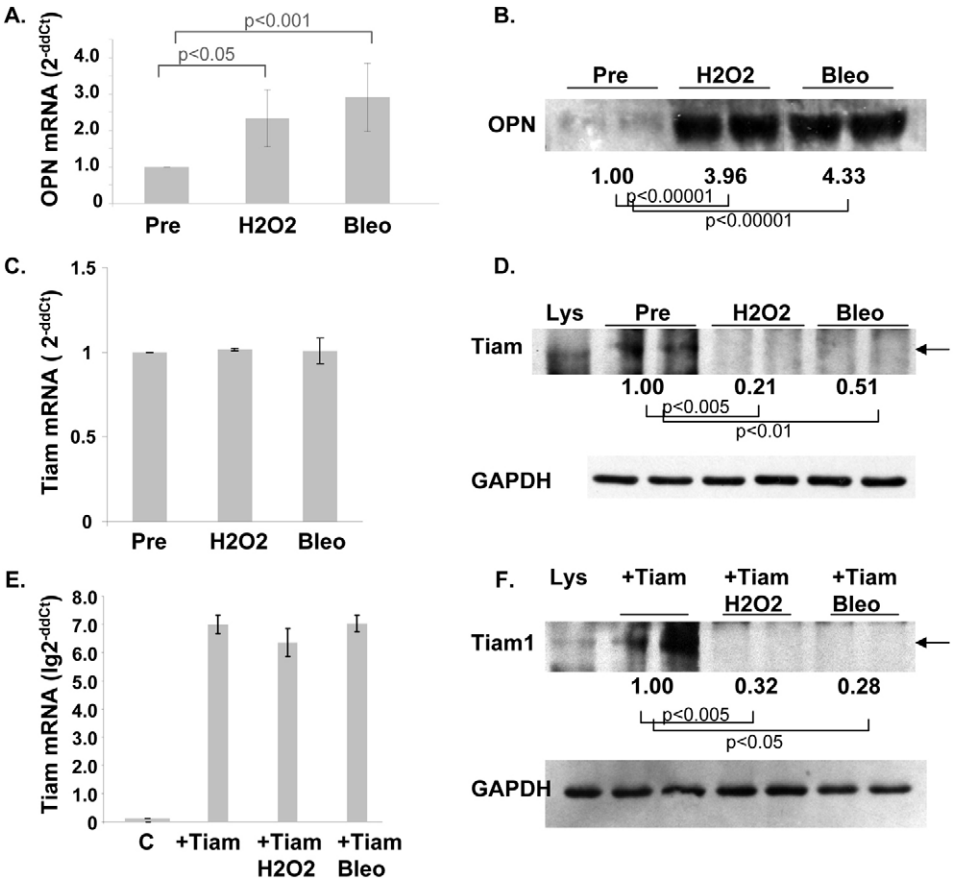

Fig. 2. Stress-induced senescence leads to inverse changes in OPN and Tiam1 in fibroblasts. (**A**,**C**,**E**) Results of qRT-PCR for *OPN* or *Tiam1* mRNA. Data indicate mean ± s.d. for at least three experiments, each done in triplicate. Results in E are rendered in log scale. (**B**,**D**,**F**) Results of immunoblots for secreted OPN (B) and Tiam1 or GAPDH as loading control in cell lysates (D,F). Numbers below immunoblots indicate quantification by densitometry for at least three experiments. Pre, pre-senescent cells; H2O2, hydrogen peroxide; Bleo, bleomycin; C, control pBabe RMF; Lys, loading control lysate for position of the full-length Tiam1 band, also indicated by an arrow. +Tiam, Tiam1-overexpressing RMF. *P* values were derived using the Student's *t*-test.

were incubated with lysates from either pre-senescent or senescent cells, and the levels of immunoprecipitated Tiam1 remaining post-incubation were assessed by immunoblotting (Fig. 3A). In cells with high levels of exogenous Tiam1, the protein often migrates on protein gels as a double band attributed to partial protein degradation. Incubation of immunoprecipitated Tiam1 with any cellular lysates led to some degradation compared with non-incubated Tiam1 precipitate (Fig. 3A, compare ratio of upper to lower bands in lane 1 with lanes 3–8). However, the overall amount of precipitated Tiam was notably decreased by incubation with lysate from senescent cells (Fig. 3A, compare lanes 3 and 6). Pre-incubation of cell lysates with either the calpain inhibitor ALLN or the calcium-chelator EDTA significantly inhibited degradation of the immobilized Tiam1 induced by senescent lysates (Fig. 3A, lanes 7 and 8, respectively). By contrast, pre-incubation of cell lysates with the proteasome inhibitor bortezomib did not prevent degradation of immobilized Tiam1 by senescent lysates (Fig. 3B, compare lanes 11 and 12 with lanes 13 and 14). These results suggest that Tiam1 downregulation in cells undergoing senescence is probably due, at least in part, to calpain-mediated protein degradation.

Tiam1 is inversely correlated with OPN expression

We hypothesized that if OPN mediates some of the effects of Tiam1 silencing, then Tiam1 levels might influence regulation of OPN expression. We therefore assessed the effect of Tiam1 overexpression on OPN levels in cells. As in Fig. 2, induction of senescence in control cells led to an increase in *OPN* mRNA (Fig. 4A, compare bars 1 and 2). In +Tiam-RMF cells, baseline levels of OPN were suppressed compared with control cells (Fig. 4A, compare bars 1 and 3). Upon induction of senescence, OPN levels did increase, but to a much lesser extent than in cells with wild-type Tiam1 expression (Fig. 4A, compare bars 2 and 4). We also verified that variation in OPN levels did not affect Tiam1 expression. In cells with stable silencing of OPN (shOPN-RMF), Tiam1 protein levels were unaffected at baseline (Fig. 4B, compare bars 1 and 3). In these cells, Tiam1 levels also decreased to a similar extent as in control cells upon senescence induction (Fig. 4B, compare bars 2 and 4). Taken together with the results shown in Fig. 1, these results show that changes in Tiam1 expression induce inverse changes in OPN secretion, suggesting that Tiam1 levels might regulate OPN secretion.

Senescent fibroblasts promote invasion and migration of associated epithelial cells

Because our data show that senescent fibroblasts have decreased Tiam1 and increased OPN, similar to levels in Tiam1-deficient fibroblasts, we then asked whether senescent fibroblasts could also promote epithelial cell invasion in three-dimensional culture. To differentiate between cell lines in mixed cell spheroid

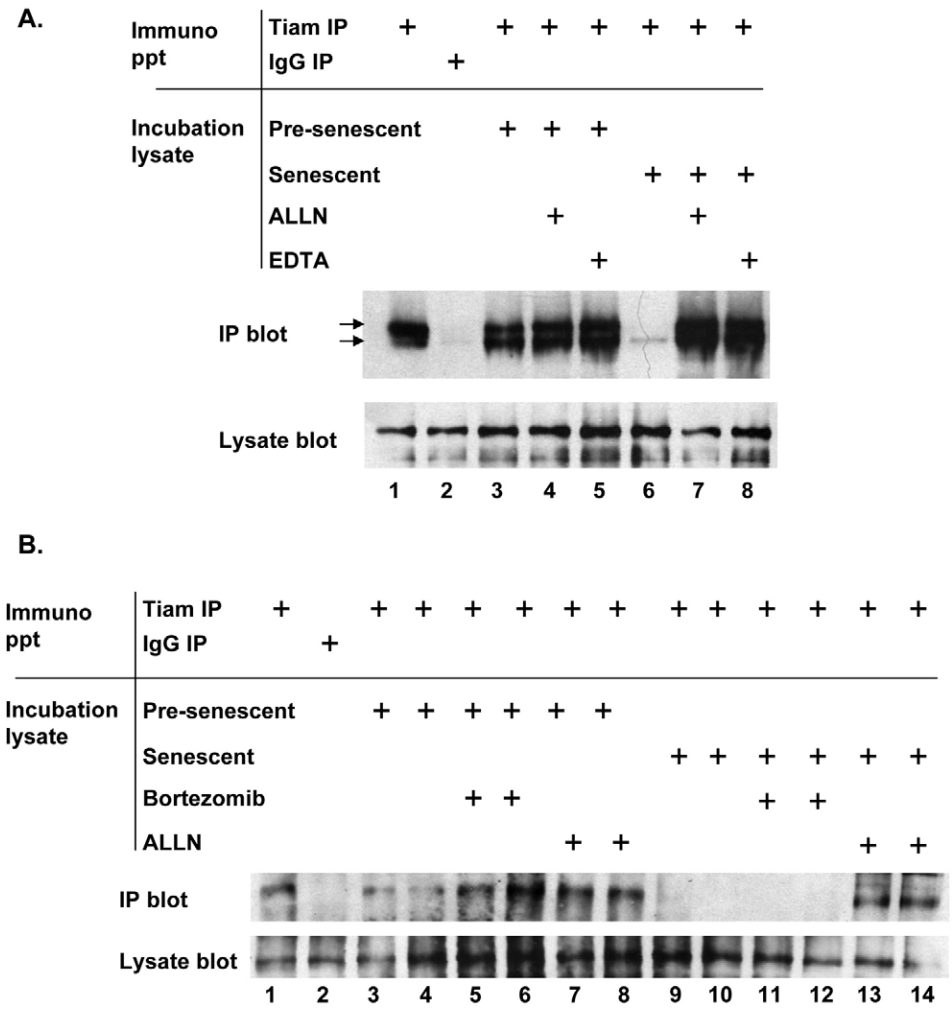

Fig. 3. Tiam1 protein is degraded by calpain protease during stress-induced senescence in cells. (**A**) IP blot: Tiam1 immunoblot of immunoprecipitates, some after incubation with lysates from pre-senescent (lanes 3–5) or senescent (lanes 6–8) cells. Some incubating lysates were pretreated with ALLN or EDTA as indicated. Arrows indicate position of upper and lower bands of precipitated Tiam1. Results are representative of two independent experiments. Lysate blot: Tiam1 immunoblot of lysates from cells with exogenous Tiam1 expression corresponding to immunoprecipitations above. (**B**) IP blot: Tiam1 immunoblot of immunoprecipitates, some after incubation with lysates from pre-senescent (lanes 3–8) or senescent (lanes 9–14) cells. Some incubating lysates were pretreated with bortezomib or ALLN as indicated. Results are representative of two independent experiments. Lysate blot: Tiam1 immunoblot of lysates from cells with exogenous Tiam1 expression corresponding to immunoprecipitations above.

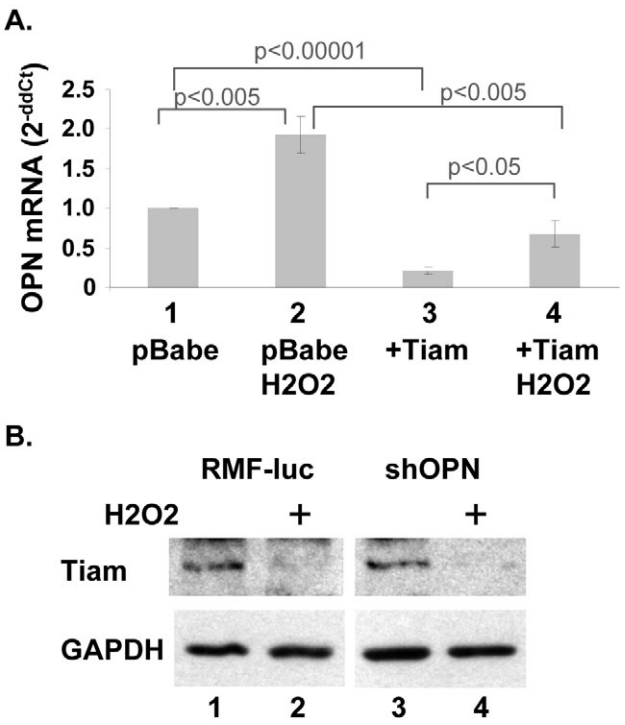

Fig. 4. Tiam1 regulates OPN expression. (**A**) qRT-PCR results for *OPN* mRNA in RMF cells with either endogenous (pBabe) or increased (+Tiam) levels of Tiam1. Results indicate mean ± s.d. for at least three experiments, each done in triplicate. *P* values were derived using the Student's *t*-test. (**B**) Immunoblots of cell lysates for Tiam1 and GAPDH from cells with either endogenous (RMF-luc) or deficient (shOPN) levels of OPN. H2O2 indicates cells rendered senescent through oxidative stress.

co-cultures, we used immortalized human mammary epithelial cells (HMECs) engineered with red fluorescence through stable expression of mCherry, and RMFs with green fluorescence through stable expression of GFP. We have previously shown that in mixed cell spheroid co-cultures with HMECs and RMFs, the fibroblasts cluster in the interior of the spheroid, whereas the epithelial cells are located around the periphery of the spheroid. Under conditions promoting increased invasiveness, HMECs form increased numbers of multicellular projections invading into the matrix (Xu et al., 2010).

In preliminary experiments, we found that HMECs exhibited increased invasiveness into the surrounding matrix when cultured with RMFs rendered senescent by exposure to either hydrogen peroxide or bleomycin, similar to the invasiveness induced upon co-culture with Tiam1-deficient fibroblasts (supplementary material Fig. S8A–D). We then optimized a protocol for isolating HMECs out of spheroid co-culture through pipetting and serial passage. This protocol yielded HMEC populations with >98% purity within 2 weeks of extraction out of co-culture, based on flow cytometry (supplementary material Fig. S9). We found that HMECs isolated after co-culture with Tiam1-deficient RMFs (termed post-co-culture HMECs) exhibited increased motility in transwell migration assays (supplementary material Fig. S8E, compare bars 1 and 4). HMECs isolated after co-culture with senescent fibroblasts also exhibited increased motility to a similar extent (supplementary material Fig. S8E, bars 2 and 3). This increased motility persisted for >12 weeks after isolation (not shown), indicating long-term effects of co-cultured fibroblasts on associated epithelial cells. (Note that for all subsequent experiments, the purity of isolated epithelial cells post-co-culture is shown in supplementary material Fig. S10).

Upregulation of Tiam1 in senescent RMF cells inhibits the invasion and migration of associated epithelial cells

Because Tiam1 expression is decreased in cells undergoing senescence, we asked whether upregulation of Tiam1 could block the increased epithelial cell invasiveness induced by senescent fibroblasts. In co-cultures of HMECs with senescent RMFs, spheroids displayed increased HMEC invasion into Matrigel, as assessed by numbers of HMEC projections per spheroid (Fig. 5A–H, compare 5C and 5G; quantified in 5Q, compare bars 1 and 2). Epithelial cells isolated from co-cultures displayed significantly increased migration when isolated from co-cultures with senescent fibroblasts compared with non-senescent fibroblasts (Fig. 5R, compare bars 1 and 2). In co-cultures of HMECs with senescent Tiam-overexpressing +Tiam-RMF cells, there was some blunting in numbers of projections per spheroid compared with senescent RMFs, with increased numbers of spheroids with 0–1 projection and decreased number of spheroids with ≥5 projections (Fig. 5I–P and 5Q, compare bars 2 and 4). In addition, although migration of HMECs isolated from co-cultures with +Tiam-RMF cells did increase with induced senescence (Fig. 5R, compare bars 3 and 4), the increase was significantly decreased compared with migration of HMECs post-co-culture with RMF cells (Fig. 5R, compare bars 2 and 4). This is consistent with the results in Fig. 4A showing that OPN increases to a much smaller degree in +Tiam1-RMF cells undergoing senescence than in control RMF cells with endogenous Tiam1 levels.

Downregulation of OPN in senescent RMF cells inhibits the invasion and migration of associated epithelial cells

We also asked whether blocking the upregulation of OPN in senescent cells would inhibit the increased epithelial cell invasiveness induced by senescent fibroblasts by performing similar experiments using an RMF line with stable silencing of OPN (shOPN-RMF). In co-cultures of HMECs with senescent shOPN-RMF there was blunting in numbers of projections per spheroid compared with senescent control RMFs, with increased numbers of spheroids with 0–1 projection and decreased number of spheroids with ≥5 projections (Fig. 6A–P, compare 6G and 6O; 6Q, compare bars 2 and 4). Migration of HMECs isolated from co-cultures with shOPN-RMF did increase with induced senescence (Fig. 6R, compare bars 3 and 4), but this increase was also significantly decreased compared with migration of HMECs post-co-culture with control RMFs (Fig. 6R, compare bars 2 and 4). These results suggest that inhibition of OPN, like upregulation of Tiam1, can partially block the increased invasiveness induced by senescent fibroblasts.

OPN mediates the effects of Tiam1 deficiency in fibroblasts on associated epithelial cells

Because OPN is a secreted glycoprotein, we asked whether we could recapitulate these results using a modified transwell migration assay. Senescent fibroblasts pre-seeded into the bottom chamber induced increased migration of HMECs across a membrane, compared with pre-senescent fibroblasts (Fig. 7A,

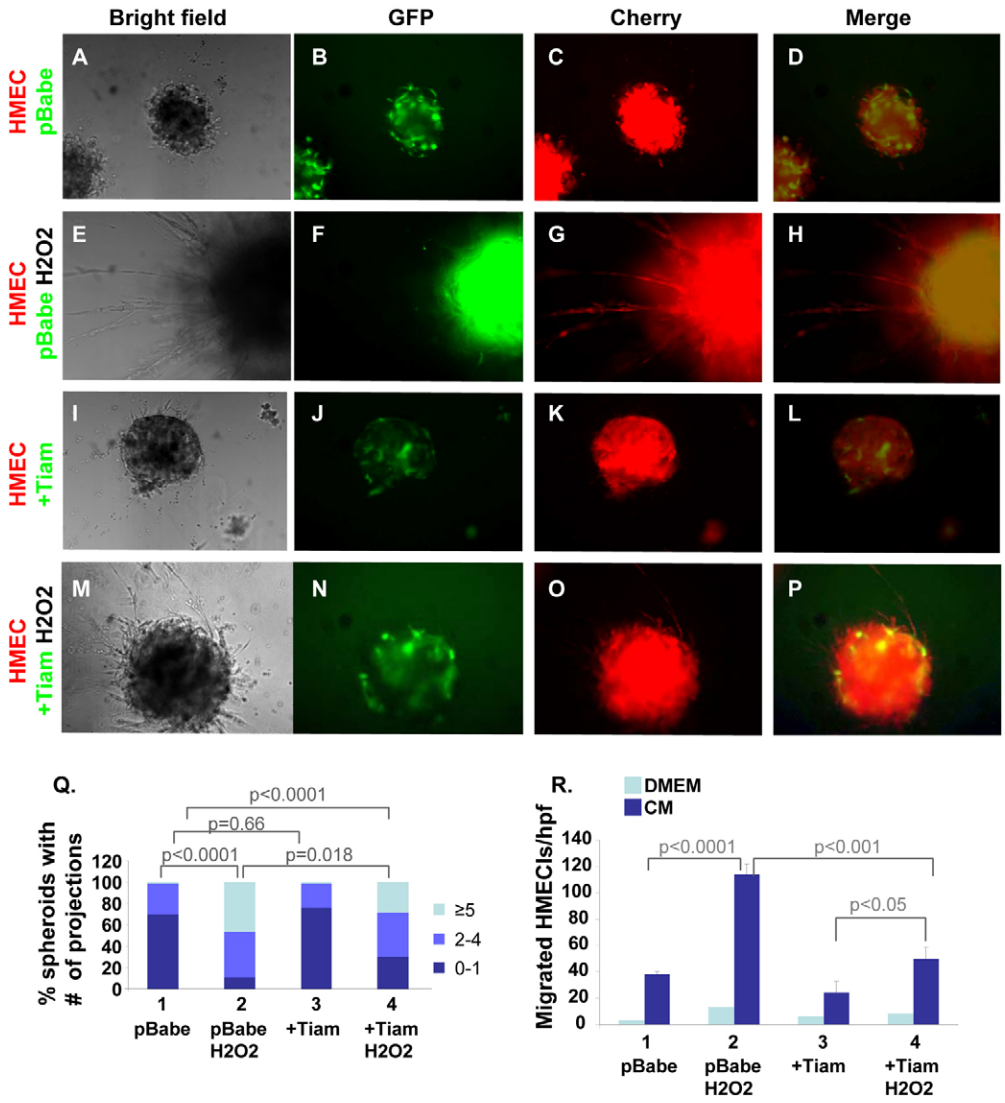

Fig. 5. Upregulation of Tiam1 in senescent RMF cells inhibits the invasion and migration of associated epithelial cells. (**A–P**) Representative images of co-cultured spheroids in Matrigel taken at 10×. Each row represents the same field and plane of focus. (A–H) Co-cultures with HMECs and control pBabe-RMFs. (I–P) Co-cultures with HMECs and Tiam-overexpressing +Tiam RMFs. (E–H,M–P) RMF cells rendered senescent prior to establishment of co-cultures. (**Q**) Numbers of spheroids with specified numbers of HMEC projections per spheroid, expressed as percentage of total spheroids. The *x*-axis indicates specific RMFs in the spheroids. Legend specifies numbers of projections per spheroid by color. Results indicate duplicate experiments; for each condition at least 25 spheroids were counted in each experiment; *P* values were determined using Chi-square. (**R**) Results of transwell migration assays on HMECs isolated from co-cultures with RMFs as indicated, expressed as mean ± s.d. Light and dark blue bars indicate migration toward bottom chamber containing DMEM or DMEM supplemented with conditioned medium, respectively. *P* values were derived using the Student's *t*-test.

compare bars 1 and 2). Fibroblasts with OPN silencing induced less migration at baseline (Fig. 7A, compare bars 1 and 3) and almost no increase in migration when rendered senescent (Fig. 7A, compare bars 3 and 4). This is consistent with the results seen using co-cultures, with decreased epithelial cell invasion into matrix and migration post-co-culture with OPN-deficient fibroblasts (Fig. 6).

We then used this assay to test the effect of inhibiting OPN secretion in Tiam1-deficient fibroblasts. Similarly to senescent fibroblasts, Tiam1-deficient fibroblasts pre-seeded in the bottom chamber induced increased migration of HMECs across a membrane compared with fibroblasts with intact Tiam1 levels (Fig. 7B, compare bars 1 and 3). Incorporation of an anti-OPN antibody into the bottom chamber blocked the increased migration induced by Tiam1-deficient fibroblasts (Fig. 7B, compare bars 3 and 4). In addition, concurrent silencing of OPN in Tiam1-deficient fibroblasts also blocked the increased migration induced by Tiam1-deficient fibroblasts (Fig. 7C, compare bars 2 and 3). This supports the idea that Tiam1 deficiency in fibroblasts promotes epithelial migration and invasion through upregulation of OPN.

Discussion

Taken together with our work on the effects of Tiam1 silencing in tumor-associated fibroblasts, these findings indicate that one mechanism by which senescent fibroblasts promote neoplastic progression in associated tumors is through degradation of fibroblast Tiam1 protein and consequent increase in fibroblast secretion of OPN. We have recently shown that Tiam1-deficient fibroblasts promote invasion and metastasis of associated epithelial tumor cells using both in vitro and in vivo models. Here we have used an in vitro three-dimensional culture model of cellular invasiveness to outline several steps underlying this effect. We find that stress-induced senescence leads to decreased levels of Tiam1 protein and increased expression of OPN, and that lysates from senescent cells induce Tiam1 protein degradation in a calcium- and calpain-dependent fashion. We also find that changes in Tiam1 protein levels lead to converse changes in *OPN* mRNA and protein secretion. Increasing the Tiam1 level in cells blunts the rise in OPN upon senescence induction. Senescent fibroblasts are able to induce increased invasion and migration in co-cultured mammary epithelial cells. These effects in the epithelial cells are ameliorated by either

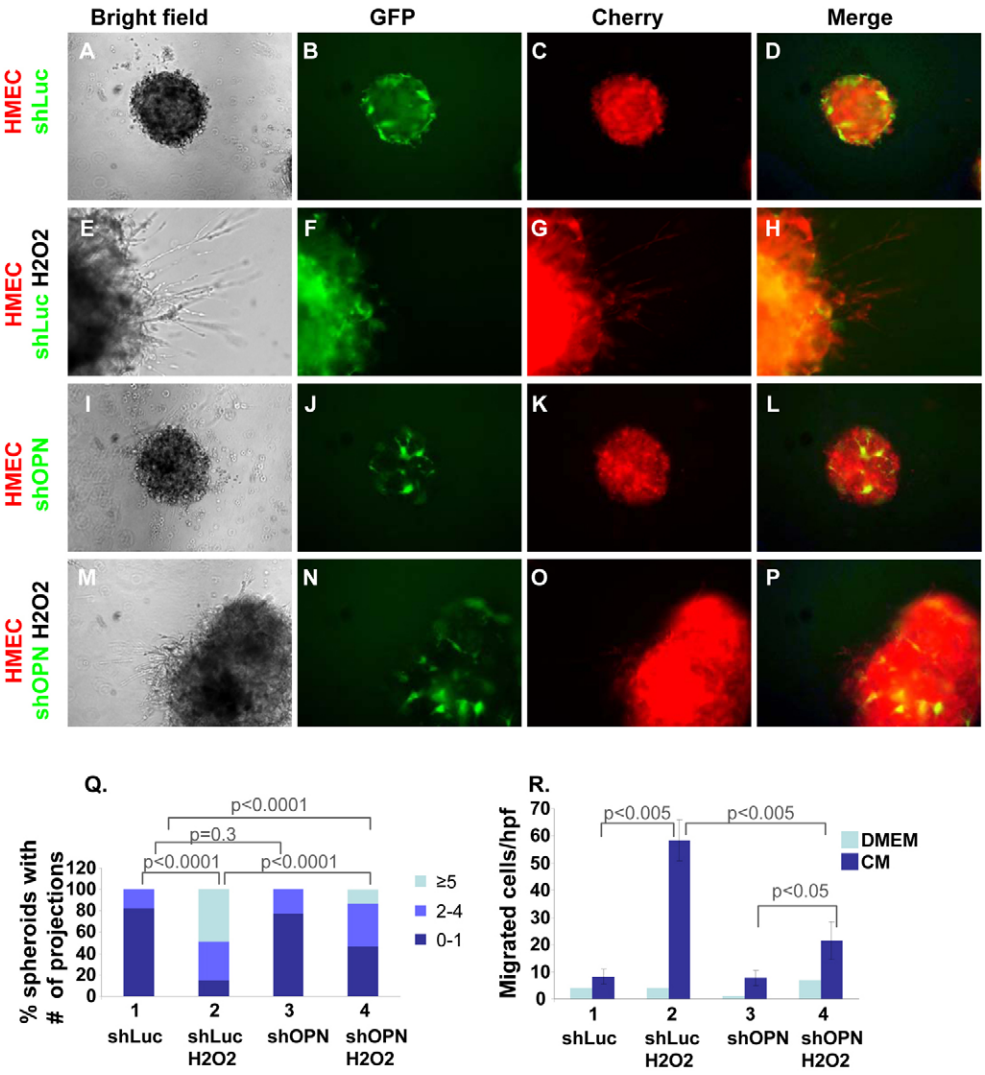

Fig. 6. Downregulation of OPN in senescent RMF cells inhibits the invasion and migration of associated epithelial cells. (**A**–**P**) Representative images of co-cultured spheroids in Matrigel taken at 10×. Each row represents the same field. (A–H) Co-cultures with HMECs and control shLuc-RMF cells. (I–P) Co-cultures with HMECs and OPN-deficient (shOPN) RMFs. (E–H,M–P) RMF cells rendered senescent prior to establishment of co-cultures. (**Q**) Numbers of spheroids with specified numbers of HMEC projections per spheroid, expressed as percentage of total spheroids, at least 25 spheroids counted in duplicated experiments; legend and statistics as in Fig. 5. (**R**) Results of transwell migration assays on HMECs isolated from co-cultures with RMFs as indicated, expressed as mean ± s.d. as in Fig. 5.

increasing levels of Tiam1 protein or decreasing OPN expression in the fibroblasts. Finally, in a seeded cell migration assay we find that either senescent fibroblasts or Tiam1-deficient fibroblasts induce increased epithelial cell migration, which was dependent on fibroblast secretion of OPN.

Although this is the first report of the effects of senescence on Tiam1 protein to our knowledge, our findings are consistent with what is known about post-transcriptional regulation of Tiam1. Tiam1 has tandem N-terminal PEST sequences, defining it as a potential target for rapid proteolytic cleavage (Rechsteiner and Rogers, 1996; Belizario et al., 2008). Tiam1 undergoes caspase-mediated cleavage in cell lines undergoing apoptosis (Qi et al., 2001). Calpain-mediated degradation was recently shown to be the probable mediator of Src-induced Tiam1 depletion localized to adherens junctions in MDCK cells (Woodcock et al., 2009). Calpains are a family of 14 calcium-regulated cysteine proteases and two regulatory proteins that initiate precise limited substrate proteolysis (Franco and Huttenlocher, 2005). Over 100 diverse calpain targets have been identified to date, indicating a wide role for calpains in mediating signal transduction processes. Calpain proteases are probably involved in the DNA damage response initiated at the start of cellular senescence, because depletion of the CAPSN1 regulatory subunit diminished senescence markers including phosphorylated histone H2AX in cells induced to undergo senescence through oncogenic, radiation or chemical stress (Demarchi et al., 2010). Our findings here indicate that calpain activity is increased in cells undergoing senescence and that Tiam1 is likely to be a calpain target in cells under those conditions. Whether this is a generalized process in senescent cells or localized to specific subcellular pools of Tiam1 remains to be determined.

Cellular senescence is thought to serve as a tumor-suppressor response in proliferating tissues that limits the replication of cells with DNA damage or telomere dysfunction and is also thought to contribute to aging (reviewed by Campisi and d'Adda di Fagagna, 2007). The number of senescent cells increases with age, and age-dependent p16-mediated suppression of progenitor cell proliferation has been demonstrated in mouse brain, bone marrow and hematopoietic tissues (Zindy et al., 1997; Janzen et al., 2006; Krishnamurthy et al., 2006; Molofsky et al., 2006). In contrast to the tumor-suppressor function of senescence, in various models of the tumor microenvironment senescent fibroblasts confer a paradoxic increase in neoplastic progression in associated tumors, with multiple cytokines,

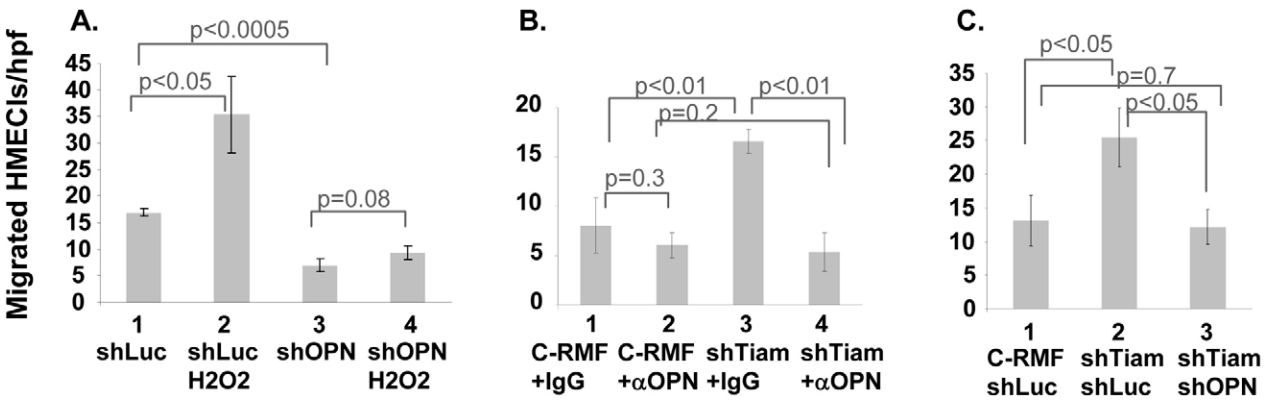

Fig. 7. OPN inhibition blocks HMEC migration induced by senescence or Tiam1 deficiency in seeded cell migration assay. HMECs were migrated across porous membranes toward bottom chambers containing (**A**) control (shLuc) or OPN-deficient (shOPN) RMFs; (**B**) control or Tiam-deficient (shTiam) RMFs; or (**C**) double hairpin control (C-RMF-shLuc), Tiam-deficient RMFs with luciferase hairpin control (shTiam-shLuc) or RMFs deficient in both Tiam1 and OPN (shTiam-shOPN). In A, H2O2 indicates RMFs rendered senescent prior to initiation of migration. In B, antibody to OPN (αOPN; bars 2 and 4) or rabbit IgG (IgG; bars 1 and 3) were added in equal amounts to bottom chambers prior to initiation of migration. *P* values were derived using the Student's *t*-test.

growth factors and matrix-altering enzymes implicated as potential mediators (Dilley et al., 2003; Parrinello et al., 2005; Bavik et al., 2006; Coppe et al., 2006). The altered pattern of gene expression exhibited by senescent cells is associated with increased secretion of inflammatory cytokines that alter the tissue microenvironment through disruption of normal architecture and stimulation of neighboring cells (Rodier et al., 2009). Because our model utilizes immortalized fibroblasts, we studied cells undergoing stress-induced senescence (SIPS) rather than replicative senescence (RS). SIPS cells and RS cells share a number of features, including morphology, SA-βgal staining, inability to replicate in response to various growth factors, similar changes in p53–p21 and $p16^{INK-4a}$ pathways, and significant similarities in gene expression patterns (Chen et al., 1995; Toussaint et al., 2000). In addition, both SIPS cells and RS fibroblasts demonstrate increased OPN and can stimulate the growth of pre-neoplastic cells (Krtolica et al., 2001; Bavik et al., 2006; Pazolli et al., 2009). Finally, the accumulation of senescent cells with aging might result from tissue damage due to oxidative stress from reactive oxygen species, suggesting considerable overlap between experimentally induced SIPS cells (especially with oxidative stress) and RS cells (Toussaint et al., 2000; Krtolica and Campisi, 2002). Our results might therefore be relevant to cells undergoing senescence as a result of aging or exposure to stressors such as chemotherapy, radiation or chronic inflammation.

Our findings indicate that increased fibroblast secretion of OPN is an important mechanism underlying the effect of senescent and/or Tiam1-deficient fibroblasts in promoting increased invasion and migration of associated mammary epithelial cells. OPN induces multiple effects in multiple cell types. In breast cancer cells, OPN is reported to regulate inhibition of apoptosis through upregulation of NFκB and PI3K pathways, increased invasiveness through upregulation of NFκB, matrix metalloproteinase-2 and urokinase plasminogen activator, and increased migration dependent on EGF and HGF receptors (reviewed by Wai and Kuo, 2004). Many OPN effects are triggered through ligation of $\alpha_v\beta$-integrin and CD44 receptor families. Tiam1 is involved in multiple signaling pathways through interactions with scaffold proteins that direct Tiam1-mediated Rac activation to specific downstream pathways (Rajagopal et al., 2010). It is likely that only a subset of Tiam1 pathways contribute to OPN regulation, because silencing the Rac GTPase does not completely phenocopy Tiam1 deficiency in fibroblasts (Xu et al., 2010). The method described here for co-culture with specific cell populations and isolating post-co-culture epithelial cells allows for systematic analysis of the effects of microenvironment fibroblasts on specific Tiam1 pathways, specific OPN receptors and potential target pathways.

In summary, we have outlined a pathway by which senescent fibroblasts in the tumor microenvironment facilitate invasiveness of associated mammary epithelial cells through degradation of fibroblast Tiam1, which leads to increased fibroblast secretion of OPN. In doing so, we have developed a technique for isolating epithelial cells exposed to microenvironment fibroblasts, which will enable future studies of specific steps involved in how Tiam1 protein levels regulate OPN, and how fibroblast OPN modulates mammary epithelial cell invasiveness. This has the potential to reveal possible targets for therapeutic inhibition of microenvironment-induced tumor invasiveness.

Materials and Methods

Cell culture

H-TERT immortalized human mammary epithelial cells (HMECs) were cultured in DME/F12 medium (HyClone) enriched with 5% bovine calf serum, 5 μg/mL insulin, 1 μg/mL hydrocortisone and 10 ng/mL EGF. H-TERT immortalized reduction mammary fibroblasts (RMFs) were grown in Dulbecco's modified Eagle's medium (DMEM) containing 10% bovine calf serum. HEK293T cells were grown in DMEM supplemented with 10% iron-supplemented bovine calf serum (Hyclone). 293FT cells for lentivirus production were grown in DMEM supplemented with 10% fetal bovine serum, 0.1 mM MEM, non-essential amino acids and 2 mM L-glutamine. MEFs were cultured in DMEM supplemented with 10% fetal bovine serum. All culture media contained 100 units/ml penicillin, 100 μg/mL of streptomycin and 0.1% fungizone. Cells were cultured in an incubator with humidified air (5% CO_2) at 37℃ in plastic dishes or otherwise as described.

For collection of RMF-conditioned medium for protein assay, RMF cells were plated at a density of 3.0×10^5 cells per 100-mm dish. Cells reached 80% confluence approximately 24 hours after being seeded, at which point the medium was replaced with serum-free medium. Conditioned medium was collected 24 hours later, concentrated 10x using VIVASPIN 20 (Sartorius Stedium, 3,000 MWCO PES) and stored at −20℃ until use.

Generation of cell lines

All oligomers used for engineering stable lines were synthesized in the Tufts DNA Core Facility. HMECs with red fluorescence through expression of mCherry, RMFs with green fluorescence through expression of eGFP, the Tiam-deficient shTiam-RMF line and the retroviral hairpin control C-RMF line have been described previously (Xu et al., 2010).

Tiam1 overexpressing +Tiam-RMF line

The cDNA for full-length Tiam1 was synthesized in two segments corresponding to base pairs 1–1948 and 1894–4773 using PCR amplification of a full-length Tiam1 cDNA template, using the following primers: 5′ segment, sense 5′-CGGG-ATCCATGGGAAACGCAGAAAGTCAA-3′ and anti-sense 5′-CCACTTTC-GTTGTCGACT-3′; 3′ segment, sense 5′-GAGCTGCCAAACCCCAAA-3′ and anti-sense 5′-ATAGTCGACGATCTCAGTGTTCAGTTTCCTC-3′.

The 5′ segment was first ligated into pBabepuro using *Bam*H1 and *Sal*1 restriction enzyme digestion, taking advantage of an internal *Sal*1 site. The 3′ segment was then ligated into the resulting product downstream of the first segment at the *Sal*1 site. Correct orientation was validated by DNA mapping and sequencing. RMF cells were then transfected with pBabepuro-Tiam1 or control pBabepuro plasmid, and stable integrants were selected by culturing in complete medium containing 0.5 μg/ml puromycin. Expression of Tiam1 in pBabepuro-Tiam1 colonies was validated by immunoblot.

Doxycycline-inducible MEF-Tiam line

The cDNA for full-length Tiam1 was cloned into the pBI-G Tet vector (Clontech) using a similar strategy as above, with the exception that the sense primer of the 5′ segment incorporated a *Not*1 site, with the following sequence: 5′ segment, sense 5′-ATAAGAAGCGGCCGCATGGGAAACGCAGAAAGTCAA-3′. The first ligation used *Not*1/*Sal*1 digestion. pBI-G-Tiam1 or pBI-G control vector were transfected into MEF/3T3 cells carrying the tetracycline-controlled transactivator tTA regulatory protein (Tet-Off; Clontech), and stable transformants were selected in hygromycin (Clontech).

OPN-deficient shOPN-RMF line

RMF lines with stable expression of short hairpin RNAs targeting OPN (shOPN-RMF) or luciferase control were generated using the pENTR/U6-pLenti6/BLOCK-iT lentiviral RNAi expression vector system (Invitrogen), using the following hairpin oligomers: OPN, sense 5′-CACCCTTTACAACAAATACCCAGATTT-CAAGAGAATCTGGGTATTTGTTGTAAAG-3′ and antisense 5′-AAAACTTTA-CAACAAATACCCAGATTCTCTTGAAATCTGGGTATTTGTTGTAAAG-3′.

For production of lentivirus, pLenti6/BLOCK-iT-OPN plasmid DNA, or pLenti6/BLOCK-iT-luci plasmid DNA, were transfected into 293FT cells along with pLP1, pLP2 and pVSV-G DNAs using Lipofectamine (Invitrogen). Virus-containing supernatant was harvested according to manufacturer's instructions. Recipient RMF cells were infected with filtered viral supernatants in the presence of 6 μg/ml polybrene, and stable transformants were selected in blasticidin (Invitrogen). Silencing of OPN in the shOPN-RMF line was verified by qRT-PCR.

Tiam and OPN-deficient shTiam-OPN-RMF line

An RMF line with stable silencing of both Tiam1 and OPN was generated by transducing the shTiam-RMF line with lentiviral particles harvested from 293FT cells transfected with the pLenti6/BLOCK-iT-OPN plasmid DNA as described above. A double viral control line with both retroviral- and lentiviral-mediated antibiotic resistance was generated by transducing the C-RMF line with lentiviral particles harvested from cells transfected with the pLenti6/BLOCK-iT-luci DNA as described above, and selected in G418 and blasticidin. Tiam1 silencing was verified by immunoblot. OPN silencing was verified by qRT-PCR.

Gene expression analysis

RNA was extracted from cell lines using the TRI reagent solution (Ambion, Austin, TX) according to manufacturer's instructions. Total RNA concentrations and RNA quality were determined using an Agilent Bioanalyzer (Agilent Technologies, Wilmington, DE), with an RNA integrity number (RIN) greater than 7 for all samples. GeneChip Human and Mouse Gene 1.0 ST Arrays (Affymetrix, Freemont, CA) were purchased for analysis of human RMF and inducible MEF lines, respectively. Microarray experiments were carried at the Yale Center for Genome Analysis, New Haven, CT. Data were analyzed in the Tufts University Center for Neuroscience Research Genomics Core facility. The GenomeStudio package (Illumina, San Diego, CA) was used to process raw expression intensity values from the GeneChips used. A number of Illumina-specified quality control parameters such as the expression of biotin, hybridization control and negative background probes were found to be consistent among the samples, indicating good quality data. Pathway analysis was performed using Ingenuity Pathways Analysis (Ingenuity Systems, Redwood City, CA).

Antibodies and Immunoblotting

Antibodies to Tiam1, OPN and glyceraldehyde 3-phosphate dehydrogenase (GAPDH) (all from Santa Cruz Biotechnology) were used according to manufacturers' instructions. Preparation of cell lysates, protein gel electrophoresis and transfer, and secondary antibodies have been previously described (Buchsbaum et al., 1996). After washing in PBS, cells were lysed in standard phosphate (SP) buffer containing 50 mM Tris pH 8.0, 120 mM NaCl, 1 mM EDTA, 0.5% NP-40 along with protease inhibitors [10 μg/ml of aprotinin, 20 μM leupeptin and 3 mM phenylmethylsulfonyl fluoride (PMSF)] and phosphatase inhibitors [50 μM sodium fluoride and 100 μM sodium orthovanadate (NaV)]. Protein bands were visualized by chemiluminescence using Western Lightning Plus-ECL Kit (PerkinElmer).

Real time PCR

Total RNA and first strand cDNA synthesis were carried out using the TRIzol and SuperScript (Invitrogen) protocols, respectively, as per manufacturer instructions. PCR was performed in triplicate reactions in 25-μl volumes containing cDNA, SYBR Green PCR Mastermix (Applied Biosystems). The primer sets used for the quantitative PCR analysis were: Tiam1 (human), sense 5′-AAGACGTA-CTCAGGCCATGTCC-3′ and antisense 5′-GACCCAAATGTCGCAGTCAG-3′; OPN (human), sense 5′-GCCATACCAGTTAAACAGGC-3′ and antisense 5′-GACCTCAGAAGATGCACTAT-3′; OPN (mouse), sense 5′-CTCCCGGTGAA-AGTGACTGA-3′ and antisense 5′-GACCTCAGAAGATGAACTCT-3′; GAPDH (human), sense 5′-CTGCACCACCAACTGCTTAG-3′ and antisense 5′-TTCAG-CTCAGGGATGACCTT-3′; β actin (mouse), sense 5′-TGGAATCCTGTGGCA-TCCATGAAAC-3′ and antisense 5′-TAAAACGCAGCTCAGTAACAGTCCG-3′.

Real-time PCR parameters used were as follows: PCR for amplification of OPN: 95℃ for 10 minutes; 95℃ for 30 seconds, 60℃ for 60 seconds and 72℃ for 60 seconds for 40 cycles. PCR for amplification of Tiam1: 94℃ for 10 minutes; 94℃ for 30 seconds, 58℃ for 40 seconds and 72℃ for 90 seconds for 45 cycles. Data analysis was done using an Opticon 2 continuous fluorescence detector (MJ Research). The 2-ΔΔ−Ct value was calculated following GAPDH or β-actin normalization.

Flow cytometry

Two to three weeks after isolation from co-culture, cells were trypsinized into single cell suspension, washed and resuspended in PBS. Cells were analyzed on a DakoCytomation New Cyan ADP using the Summit 4.3 program, with *x*-axis set to FITC Log Comp to detect cells containing eGFP and *y*-axis set to PE-Texas Red Log Comp to detect cells containing mCherry.

Transwell migration assays

Cultured cells were deprived of serum overnight, trypsinized and plated at a density of 1×10^5 cells/ml (2×10^4 cells/basket) in the upper basket of transwell chambers with a filter pore size of 8 μm (Costar). Cells were allowed to migrate for 5 hours at 37℃ toward lower chambers containing either DMEM alone or DMEM supplemented with 25% filter-sterilized conditioned medium harvested from NIH3T3 cells. Non-migrated cells were then removed from the upper side of the filter using a cotton swab. Filters were fixed and stained with the Protocol 3 HEMA Stain kit (Fisher). Filters were cut out and mounted on glass slides under coverslips using Resolve microscope immersion oil (Richard Allen Scientific). Migrated cells were counted in nine random fields using a Nikon Eclipse TS100 microscope and 20× objective.

Seeded cell migration assay

Indicated RMF cells were seeded on the bottom of the lower chamber 1 day before the migration assay at a density of 2×10^4 cells/chamber and were returned to the incubator overnight to reach approximately 70% confluence. Where indicated, OPN antibody (Santa Cruz Biotechnology) or rabbit IgG were added to the lower chamber at a concentration of 1 μg/ml immediately after RMFs were seeded.

Senescence induction and SA-βgal staining

To induce senescence, 2.5×10^5 RMF cells were seeded on 100-mm plates for 48 hours until approximately 80% confluent and then treated with either 800 μmol/L hydrogen peroxide for 2 hours or 50 μg/ml bleomycin in culture medium for 24 hours at 37℃. After treatment, cells were rinsed twice with PBS and left to recover in culture medium. For radiation-induced senescence, cells were subjected to 16 Gy X-irradiation (233 cGy/minute for 6 minutes 52 seconds) and returned to the incubator to recover. For each treatment, senescence induction was repeated 3–5 days later to prevent recovery and cell cycle re-entry. Cells were subcultured for at least 7 days and senescence induction was confirmed by ≥90% SA-βgal staining.

SA-βgal staining

SA-βgal staining was conducted as described previously (Dimri et al., 1995). Briefly, cells were washed twice in PBS and fixed for 5 minutes in 2%

formaldehyde and 0.2% glutaraldehyde, washed again and incubated at 37℃ overnight with fresh SA-βgal stain solution: 1 mg/ml 5-bromo-4-chloro-3-indolyl-β-D-galactoside (X-Gal) (stock solution was 20 mg/ml in dimethylformamide), 40 mM citric acid/sodium phosphate pH 6.0, 5 mM potassium ferrocyanide, 5 mM potassium ferricyanide, 150 mM NaCl and 2 mM $MgCl_2$. Cells with positive staining were observed and counted under a light microscope (Nikon, Eclipse TS100).

Calpain activity assay

Calpain activation was assessed by fluorometric detection of cleavage of calpain substrate using a purchased Calpain Activity Assay Kit (Biovision Research Products) according to manufacturer's instructions. Briefly, equal numbers of cells were lysed in supplied extraction buffer, and post-centrifugation supernatants were normalized for protein content in extraction buffer. After addition of the supplied reaction buffer and calpain substrate (Ac-LLY-AFC), samples were incubated in the dark for 1 hour at 37℃. Samples were transferred to 96-well plates and fluorescence was detected using a Victor3 V1420 Multilabel Counter and Wallac Victor 3V software (PerkinElmer) equipped with a 405 nm excitation filter and 535 nm emission filter. Results were corrected for background fluorescence as measured in empty wells. In some samples, calpain substrate was omitted (negative control), supplied calpain inhibitor was added, or supplied active calpain was added to extraction buffer (positive control).

In vitro Tiam1 cleavage assay

Tiam1 immunoprecipitation

HEK293T cells were transiently transfected with full-length Tiam1 cDNA as previously described (Buchsbaum et al., 2002). At 48 hours after transfection, cells were washed once with PBS and lysed in SP buffer as described above. Lysates were cleared of unbroken cells and debris by centrifugation at 10,000 ***g*** for 10 minutes. Aliquots of cleared lysates were reserved for immunoblotting; the remainder were incubated with protein A-Sepharose beads (Pharmacia) and anti-Tiam1 antibody (diluted according to the manufacturer's instructions) or equal amounts of polyclonal rabbit IgG (Santa Cruz Biotechnology) for 2 hours at 4℃ with constant agitation. Immunoprecipitates were washed twice with ice-cold SP buffer and once with reaction buffer (20 mM Tris-HCl pH 7.5, 10 mM DTT and 6 mM $CaCl_2$) in the presence of protease inhibitors (1 mM PMSF and 1.7 µg/ml aprotinin) prior to the cleavage reaction.

Preparation of extracted lysates from pre-senescent and senescent RMF cells

Pre-senescent cells were maintained in culture as described above. Senescence was induced with 800 µM H_2O_2 as described above, and confirmed by SA-βgal staining. Pre-senescent and senescent RMFs were washed with cold PBS, pelleted and resuspended in extraction buffer (10 mM HEPES pH 7.0, 2 mM $MgCl_2$, 50 mM NaCl and 1 mM DTT) containing inhibitors (17 µg/ml aprotinin, 10 µg/ml leupepsin, 100 µM NaV and 3.3 mM PMSF). Cells were lysed by freeze–thaw cycles in ethanol–liquid nitrogen and a 37℃ water bath. Extracts were centrifuged at 10,000 ***g*** for 15 minutes at 4℃, and resulting supernatants were used as the cytosolic fraction. Protein concentration was determined by BCA protein assay (Bio-Rad).

Cleavage reaction

Immunoprecipitated proteins were incubated with extracted lysates from pre-senescent or senescent cells in reaction buffer for 2 hours at 37℃ with constant agitation. Where indicated, extracted lysates were pre-incubated on ice for 30 minutes with calpain inhibitor (50 µM ALLN) or 1 mM EDTA, or with proteasome inhibitor (5 nM bortezomib) for 37℃ for 24 hours before the cleavage reaction. Proteasome inhibition under these conditions was verified using the Proteasome-Glo Cell-Based Assay and GloMax–multi+Detection system (Promega) according to manufacturer's instructions. The beads were then washed three times with Tris-HCl pH 7.5 and the reaction was stopped by addition of 6× Laemmli buffer and heating. Samples were resolved by SDS-PAGE and immunoblotting as described.

Spheroid co-culture in Matrigel

As described previously (Xu et al., 2010), Matrigel (BD Biosciences) was diluted 1:1 with ice-cold HMEC medium, and 50 µl of the mixture was placed mid-well in a 24-well plate. After incubating for 5 minutes at 37℃, an additional 250 µl of Matrigel–medium mixture was added into the well and incubated for another 30 minutes. A 1:1 mixture of HMEC and RMF cells (0.5×10^5 cells each) in 0.5 ml of HMEC medium was gently dropped onto the top of the solidified gel. Cells were cultured for 2 weeks and medium was changed every 2–3 days. Spheroid formation and projection growth were monitored daily under light microscopy. Images were obtained on a Diaphot Software Version 4.1 (Diagnostic Instruments).

Isolation of cells from spheroid co-culture

Co-cultured spheroids were removed from Matrigel by gentle pipetting using 1000 µl plastic pipette tips with the tip cut off, transferred to sterile 15 ml centrifuge tubes and centrifuged at 2000 r.p.m. (350 ***g***) for 5 minutes. The disrupted Matrigel was gently removed from the top of the tubes and the pelleted cells and spheroids were transferred in HMEC medium to 35-mm wells. Cell–spheroid mixtures were cultured for 7–10 days until cells lost the spheroid structure and became monolayers, and then expanded when reaching 50% confluence.

Conflict of interest

The authors declare no conflict of interest.

Funding

This work was supported by the National Cancer Institute [grant number RO1CA095559 to R.J.B.], the Landmann Family Fund of the Vermont Community Foundation (to R.J.B.), the Tufts Medical Center Diane Connolly-Zaniboni Scholarship in Breast Cancer (to R.J.B.), the China Scholarship Council State Scholarship Fund [grant number 2008624080 to J.L.], the Tufts Center for Neuroscience Research [grant number P30NS047423] and the National Institutes of Health [grant number 5R25HL007785 to M.C.]. Deposited in PMC for release after 12 months.

Supplementary material available online at
http://jcs.biologists.org/lookup/suppl/doi:10.1242/jcs.089466/-/DC1

References

Aoshiba, K., Tsuji, T. and Nagai, A. (2003). Bleomycin induces cellular senescence in alveolar epithelial cells. *Eur. Respir. J.* **22**, 436-443.

Bavik, C., Coleman, I., Dean, J. P., Knudsen, B., Plymate, S. and Nelson, P. S. (2006). The gene expression program of prostate fibroblast senescence modulates neoplastic epithelial cell proliferation through paracrine mechanisms. *Cancer Res.* **66**, 794-802.

Belizario, J. E., Alves, J., Garay-Malpartida, M. and Occhiucci, J. M. (2008). Coupling caspase cleavage and proteasomal degradation of proteins carrying PEST motif. *Curr. Protein Pept. Sci.* **9**, 210-220.

Ben-Porath, I. and Weinberg, R. A. (2005). The signals and pathways activating cellular senescence. *Int. J. Biochem. Cell Biol.* **37**, 961-976.

Buchsbaum, R., Telliez, J. B., Goonesekera, S. and Feig, L. A. (1996). The N-terminal pleckstrin, coiled-coil, and IQ domains of the exchange factor Ras-GRF act cooperatively to facilitate activation by calcium. *Mol. Cell. Biol.* **16**, 4888-4896.

Buchsbaum, R. J., Connolly, B. A. and Feig, L. A. (2002). Interaction of Rac exchange factors Tiam1 and Ras-GRF1 with a scaffold for the p38 mitogen-activated protein kinase cascade. *Mol. Cell. Biol.* **22**, 4073-4085.

Buchsbaum, R. J., Connolly, B. A. and Feig, L. A. (2003). Regulation of p70 S6 kinase by complex formation between the Rac guanine nucleotide exchange factor (Rac-GEF) Tiam1 and the scaffold spinophilin. *J. Biol. Chem.* **278**, 18833-18841.

Campisi, J. (2005). Senescent cells, tumor suppression, and organismal aging: good citizens, bad neighbors. *Cell* **120**, 513-522.

Campisi, J. and d'Adda di Fagagna, F. (2007). Cellular senescence: when bad things happen to good cells. *Nat. Rev. Mol. Cell. Biol.* **8**, 729-740.

Castro, P., Giri, D., Lamb, D. and Ittmann, M. (2003). Cellular senescence in the pathogenesis of benign prostatic hyperplasia. *Prostate* **55**, 30-38.

Chen, Q., Fischer, A., Reagan, J. D., Yan, L. J. and Ames, B. N. (1995). Oxidative DNA damage and senescence of human diploid fibroblast cells. *Proc. Natl. Acad. Sci. USA* **92**, 4337-4341.

Connolly, B. A., Rice, J., Feig, L. A. and Buchsbaum, R. J. (2005). Tiam1-IRSp53 complex formation directs specificity of rac-mediated actin cytoskeleton regulation. *Mol. Cell. Biol.* **25**, 4602-4614.

Coppe, J. P., Kauser, K., Campisi, J. and Beausejour, C. M. (2006). Secretion of vascular endothelial growth factor by primary human fibroblasts at senescence. *J. Biol. Chem.* **281**, 29568-29574.

Coppe, J. P., Patil, C. K., Rodier, F., Sun, Y., Munoz, D. P., Goldstein, J., Nelson, P. S., Desprez, P. Y. and Campisi, J. (2008). Senescence-associated secretory phenotypes reveal cell-nonautonomous functions of oncogenic RAS and the p53 tumor suppressor. *PLoS Biol.* **6**, 2853-2868.

d'Adda di Fagagna, F., Reaper, P. M., Clay-Farrace, L., Fiegler, H., Carr, P., Von Zglinicki, T., Saretzki, G., Carter, N. P. and Jackson, S. P. (2003). A DNA damage checkpoint response in telomere-initiated senescence. *Nature* **426**, 194-198.

Davalos, A. R., Coppe, J. P., Campisi, J. and Desprez, P. Y. (2010). Senescent cells as a source of inflammatory factors for tumor progression. *Cancer Metastasis Rev.* **29**, 273-283.

Demarchi, F., Cataldo, F., Bertoli, C. and Schneider, C. (2010). DNA damage response links calpain to cellular senescence. *Cell Cycle* **9**, 755-760.

Dilley, T. K., Bowden, G. T. and Chen, Q. M. (2003). Novel mechanisms of sublethal oxidant toxicity: induction of premature senescence in human fibroblasts confers tumor promoter activity. *Exp. Cell Res.* **290**, 38-48.

Dimri, G. P., Lee, X., Basile, G., Acosta, M., Scott, G., Roskelley, C., Medrano, E. E., Linskens, M., Rubelj, I., Pereira-Smith, O. et al. (1995). A biomarker that identifies senescent human cells in culture and in aging skin in vivo. *Proc. Natl. Acad. Sci. USA* **92**, 9363-9367.

Franco, S. J. and Huttenlocher, A. (2005). Regulating cell migration: calpains make the cut. *J. Cell Sci.* **118**, 3829-3838.

Hayflick, L. (1965). The limited in vitro lifetime of human diploid cell strains. *Exp. Cell Res.* **37**, 614-636.

Hornsby, P. J. (2007). Senescence as an anticancer mechanism. *J. Clin. Oncol.* **25**, 1852-1857.

Itahana, K., Campisi, J. and Dimri, G. P. (2004). Mechanisms of cellular senescence in human and mouse cells. *Biogerontology* **5**, 1-10.

Janzen, V., Forkert, R., Fleming, H. E., Saito, Y., Waring, M. T., Dombkowski, D. M., Cheng, T., DePinho, R. A., Sharpless, N. E. and Scadden, D. T. (2006). Stem-cell ageing modified by the cyclin-dependent kinase inhibitor p16INK4a. *Nature* **443**, 421-426.

Juo, P., Kuo, C. J., Yuan, J. and Blenis, J. (1998). Essential requirement for caspase-8/FLICE in the initiation of the Fas-induced apoptotic cascade. *Curr. Biol.* **8**, 1001-1008.

Kang, J., Chen, W., Xia, J., Li, Y., Yang, B., Chen, B., Sun, W., Song, X., Xiang, W., Wang, X. et al. (2008). Extracellular matrix secreted by senescent fibroblasts induced by UVB promotes cell proliferation in HaCaT cells through PI3K/AKT and ERK signaling pathways. *Int. J. Mol. Med.* **21**, 777-784.

Krishnamurthy, J., Ramsey, M. R., Ligon, K. L., Torrice, C., Koh, A., Bonner-Weir, S. and Sharpless, N. E. (2006). p16INK4a induces an age-dependent decline in islet regenerative potential. *Nature* **443**, 453-457.

Krtolica, A. and Campisi, J. (2002). Cancer and aging: a model for the cancer promoting effects of the aging stroma. *Int. J. Biochem. Cell. Biol.* **34**, 1401-1414.

Krtolica, A., Parrinello, S., Lockett, S., Desprez, P. Y. and Campisi, J. (2001). Senescent fibroblasts promote epithelial cell growth and tumorigenesis: a link between cancer and aging. *Proc. Natl. Acad. Sci. USA* **98**, 12072-12077.

Li, H., Bergeron, L., Cryns, V., Pasternack, M. S., Zhu, H., Shi, L., Greenberg, A. and Yuan, J. (1997). Activation of caspase-2 in apoptosis. *J. Biol. Chem.* **272**, 21010-21017.

Mertens, A. E., Roovers, R. C. and Collard, J. G. (2003). Regulation of Tiam1-Rac signalling. *FEBS Lett.* **546**, 11-16.

Molofsky, A. V., Slutsky, S. G., Joseph, N. M., He, S., Pardal, R., Krishnamurthy, J., Sharpless, N. E. and Morrison, S. J. (2006). Increasing p16INK4a expression decreases forebrain progenitors and neurogenesis during ageing. *Nature* **443**, 448-452.

Narita, M., Nunez, S., Heard, E., Lin, A. W., Hearn, S. A., Spector, D. L., Hannon, G. J. and Lowe, S. W. (2003). Rb-mediated heterochromatin formation and silencing of E2F target genes during cellular senescence. *Cell* **113**, 703-716.

Parrinello, S., Coppe, J. P., Krtolica, A. and Campisi, J. (2005). Stromal-epithelial interactions in aging and cancer: senescent fibroblasts alter epithelial cell differentiation. *J. Cell Sci.* **118**, 485-496.

Pazolli, E., Luo, X., Brehm, S., Carbery, K., Chung, J. J., Prior, J. L., Doherty, J., Demehri, S., Salavaggione, L., Piwnica-Worms, D. et al. (2009). Senescent stromal-derived osteopontin promotes preneoplastic cell growth. *Cancer Res.* **69**, 1230-1239.

Qi, H., Juo, P., Masuda-Robens, J., Caloca, M. J., Zhou, H., Stone, N., Kazanietz, M. G. and Chou, M. M. (2001). Caspase-mediated cleavage of the TIAM1 guanine nucleotide exchange factor during apoptosis. *Cell Growth Differ.* **12**, 603-611.

Rajagopal, S., Ji, Y., Xu, K., Li, Y., Wicks, K., Liu, J., Wong, K. W., Herman, I. M., Isberg, R. R. and Buchsbaum, R. J. (2010). Scaffold proteins IRSp53 and spinophilin regulate localized Rac activation by T-lymphocyte invasion and metastasis protein 1 (TIAM1). *J. Biol. Chem.* **285**, 18060-18071.

Rechsteiner, M. and Rogers, S. W. (1996). PEST sequences and regulation by proteolysis. *Trends Biochem. Sci.* **21**, 267-271.

Rodier, F., Coppe, J. P., Patil, C. K., Hoeijmakers, W. A., Munoz, D. P., Raza, S. R., Freund, A., Campeau, E., Davalos, A. R. and Campisi, J. (2009). Persistent DNA damage signalling triggers senescence-associated inflammatory cytokine secretion. *Nat. Cell Biol.* **11**, 973-979.

Toussaint, O., Medrano, E. E. and von Zglinicki, T. (2000). Cellular and molecular mechanisms of stress-induced premature senescence (SIPS) of human diploid fibroblasts and melanocytes. *Exp. Gerontol.* **35**, 927-945.

Wai, P. Y. and Kuo, P. C. (2004). The role of osteopontin in tumor metastasis. *J. Surg. Res.* **121**, 228-241.

Wai, P. Y. and Kuo, P. C. (2008). Osteopontin: regulation in tumor metastasis. *Cancer Metastasis Rev.* **27**, 103-118.

Weber, G. F. (2008). Molecular mechanisms of metastasis. *Cancer Lett.* **270**, 181-190.

Woodcock, S. A., Rooney, C., Liontos, M., Connolly, Y., Zoumpourlis, V., Whetton, A. D., Gorgoulis, V. G. and Malliri, A. (2009). SRC-induced disassembly of adherens junctions requires localized phosphorylation and degradation of the rac activator tiam1. *Mol. Cell* **33**, 639-653.

Xu, K., Rajagopal, S., Klebba, I., Dong, S., Ji, Y., Liu, J., Kuperwasser, C., Garlick, J. A., Naber, S. P. and Buchsbaum, R. J. (2010). The role of fibroblast Tiam1 in tumor cell invasion and metastasis. *Oncogene* **29**, 6533-6542.

Yang, G., Rosen, D. G., Zhang, Z., Bast, R. C., Jr., Mills, G. B., Colacino, J. A., Mercado-Uribe, I. and Liu, J. (2006). The chemokine growth-regulated oncogene 1 (Gro-1) links RAS signaling to the senescence of stromal fibroblasts and ovarian tumorigenesis. *Proc. Natl. Acad. Sci. USA* **103**, 16472-16477.

Zhang, H. and Macara, I. G. (2006). The polarity protein PAR-3 and TIAM1 cooperate in dendritic spine morphogenesis. *Nat. Cell Biol.* **8**, 227-237.

Zindy, F., Quelle, D. E., Roussel, M. F. and Sherr, C. J. (1997). Expression of the p16INK4a tumor suppressor versus other INK4 family members during mouse development and aging. *Oncogene* **15**, 203-211.